

Use of Elastic-Scattering Parameters in  $(d,p)$  Stripping Calculations\*

WILLIAM R. SMITH

Oak Ridge National Laboratory, Oak Ridge, Tennessee

(Received 8 October 1964)

The angular distributions of  $^{90}\text{Zr}(d,p)^{91}\text{Zr}$ ,  $^{52}\text{Cr}(d,p)^{53}\text{Cr}$ ,  $^{206}\text{Pb}(d,p)^{207}\text{Pb}$ , and  $\text{Zn}(d,p)$  were calculated by means of the distorted-wave Born approximation in which various optical-model parameter sets were obtained by fitting appropriate deuteron and proton elastic-scattering data. In most cases it was found that parameter ambiguities did not greatly affect the relative angular distributions, but did cause differences of more than a factor of 2 between the resulting spectroscopic factors. Potential ambiguities of the form  $VR^n = \text{const}$  were shown to be of considerably greater importance for the stripping results than were other types of ambiguities.

## INTRODUCTION

SEVERAL investigations<sup>1-4</sup> have shown that distorted-wave Born approximation (DWBA) calculations of  $(d,p)$  distributions give results in substantial agreement with experiment when medium or heavy targets are used. In principle the optical-model parameters to be used in such calculations should resemble those which yield agreement with the appropriate experimental deuteron and proton elastic-scattering data. However, it is well known that a given elastic-scattering angular distribution can usually be fitted by any one of many different sets of parameters.<sup>5-8</sup> For instance, a range of radii  $R$  and potential depths  $V$  obeying the relationship  $VR^n = \text{constant}$  ( $2 \leq n \leq 3$ ) can almost always be found that produces very similar fits to the elastic scattering. For deuteron scattering, nearly identical fits are also obtained when the "constant" in the preceding equation takes on any one of a series of discrete values.<sup>7,8</sup> It is therefore of interest to determine how sensitive the stripping results are to different choices of acceptable elastic-scattering parameters. For this purpose,  $(d,p)$  reactions employing  $^{90}\text{Zr}$ ,  $^{52}\text{Cr}$ ,  $^{206}\text{Pb}$ , and  $\text{Zn}$  as targets have been investigated.

The distorted-wave theory upon which the present calculations are based is known to be incomplete. Explicitly, it does not include such effects as spin-orbit or tensor interactions,<sup>9</sup> a finite-range neutron-proton interaction,<sup>10</sup> nonlocal potentials,<sup>11</sup> collective effects,<sup>12</sup>

antisymmetrization of the total wave function,<sup>13</sup> the influence of the target on the deuteron internal wave function,<sup>14</sup> the deuteron polarizability or breakup,<sup>15</sup> the compound-nucleus interference or decay,<sup>16</sup> or the residual proton-target interaction.<sup>17</sup> The main point under investigation here is the study of the dependence of the stripping on the choice of *a priori* acceptable parameter sets. Due to the fair degree of success enjoyed by the simplified form of the theory, it seems reasonable to suppose that the most important physical processes entering the reaction are accounted for and that the variations in the results obtained by its use will, at least crudely, be indicative of what to expect if a more accurate theory were used.

An estimate of how much the results may be changed by more precise calculations is already available in several cases. Thus, the inclusion of spin-orbit interactions in the deuteron and proton channels seriously modifies the relative angular distributions at large angles but not at forward angles, and the absolute magnitude of the stripping peak may be changed by amounts varying from zero to 20%.<sup>18</sup> The combined use of a finite-range neutron-proton potential and of nonlocal potentials for the remaining interactions serves to reduce the amount of stripping occurring in the nuclear interior by approximately 50%,<sup>19</sup> so that with their inclusion, variations in stripping results that arise from using wave functions which differ from one another mainly in the nuclear interior may be expected to undergo a reduction of similar magnitude. The neglect of modifications to the deuteron internal structure as it passes through the nucleus may well be the weakest point in the theory. Unfortunately, other than the deuteron's breakup being accounted for by the

\* Research sponsored by the U. S. Atomic Energy Commission under contract with the Union Carbide Corporation.

<sup>1</sup> W. Tobocman, Phys. Rev. **115**, 99 (1959); S. Hinds, R. Middleton, and D. J. Pullen, Phys. Letters **1**, 12 (1962).

<sup>2</sup> D. W. Miller, H. E. Wegner, and W. S. Hall, Phys. Rev. **125**, 2054 (1962).

<sup>3</sup> P. T. Andrews *et al.*, Phys. Letters **3**, 97 (1963).

<sup>4</sup> W. R. Smith and E. V. Ivash, Phys. Rev. **128**, 1175 (1962).

<sup>5</sup> J. S. Nodvik and D. S. Saxon, Phys. Rev. **117**, 1539 (1960).

<sup>6</sup> F. G. Perey, Phys. Rev. **131**, 745 (1963).

<sup>7</sup> C. M. Perey and F. G. Perey, Phys. Rev. **132**, 755 (1963).

<sup>8</sup> E. C. Halbert, Nucl. Phys. **50**, 353 (1964).

<sup>9</sup> D. Robson, Nucl. Phys. **22**, 34 (1961); G. R. Satchler, *ibid.* **21**, 116 (1960).

<sup>10</sup> N. Austern, R. M. Drisko, E. C. Halbert, and G. R. Satchler, Phys. Rev. **133**, B3 (1964).

<sup>11</sup> F. G. Perey and B. Buck, Nucl. Phys. **32**, 353 (1962).

<sup>12</sup> S. K. Penny and G. R. Satchler, Nucl. Phys. **53**, 145 (1964); J. A. Sawicki and G. R. Satchler, *ibid.* **7**, 289 (1958).

<sup>13</sup> W. Tobocman, *Theory of Direct Nuclear Reactions* (Oxford University Press, New York, 1961).

<sup>14</sup> C. F. Clement, Phys. Rev. **128**, 2728 (1962); R. J. Drachman, *ibid.* **132**, 374 (1963).

<sup>15</sup> A. I. Akhiezer and A. G. Sitenko, Phys. Rev. **106**, 1236 (1957); R. Gold and C. Wong, *ibid.* **132**, 2586 (1963).

<sup>16</sup> R. G. Thomas, Phys. Rev. **100**, 25 (1955).

<sup>17</sup> F. S. Levin, Brookhaven National Laboratory Report No. BNL-7548, 1963 (unpublished).

<sup>18</sup> L. L. Lee, Jr., J. P. Schiffer, B. Zeidman, G. R. Satchler, R. M. Drisko, and R. H. Bassel, Phys. Rev. **136**, B971 (1964).

<sup>19</sup> F. G. Perey and G. R. Stachler (private communication).

absorptive potential, it is not known at present either how to include such effects properly or how much they can be expected to change the outcome of the calculations.

Three things which may in principle be determined by means of distorted-wave ( $d,p$ ) stripping calculations are (1) reaction mechanisms, (2) optical-model parameters, and (3) spectroscopic factors. As a practical matter, however, a problem is created by the incompatibility between (1) and (2). In order to study (1) one must know (2), and vice versa. Further, in order to study (3) one must know both (1) and (2). These problems come about because one does not know which set of optical model parameters to use in the calculation. The parameters should certainly yield fits to the appropriate elastic-scattering data. However, as noted before, a given set of elastic-scattering data can, if fitted at all, be adequately fitted by using any one of many different sets of parameters. Although these different parameter sets may yield similar elastic-scattering results, they will give stripping results which differ by varying degrees.

Several reasons for expecting these differences exist. First, the stripping depends on the shapes of the wave functions in the nuclear interior, whereas the elastic scattering depends only on the logarithmic derivatives of the radial wave functions at the nuclear surface. Second, the relative importance of the various partial waves may not be the same for stripping as for elastic scattering, so that parameter sets which cause differences in partial waves unimportant in elastic scattering may generate sizable variations in the stripping results. And third, the energies and isotopes (or isotopic mixtures) involved in the elastic scattering may not be the same as those used in the stripping, so that even if different parameter sets did yield identical wave functions in one case they would be expected to yield somewhat different wave functions in the other case (this is the usual situation encountered in stripping studies).

Another source of difficulty in evaluating stripping results arising from the use of elastic-scattering parameters is that possible errors in the elastic-scattering data may cause the wave functions generated in fitting the data to differ from the wave functions that would be obtained if precise data were used. There are several situations which may be classified as errors of this type: (1) Errors in the relative angular distributions; these are serious when the bombarding energy is near the Coulomb barrier height so that the angular distribution does not differ greatly from Rutherford scattering and hence the parameters are determined by fitting rather small structural features, the exact nature of which could be seriously affected by moderate errors in the data; (2) the absence of, or an erroneous determination of, the absolute cross section; (3) energy-dependent fluctuations of the cross section; and (4)

the use of mixed isotopes, or of the wrong isotope. The study of the effects of such errors on the stripping results is important because in some cases relatively small errors in the elastic scattering may seriously affect the stripping. The possibility of such errors also weakens the criterion that only best-fit elastic-scattering parameters should be used in stripping calculations.

Returning now to information obtainable from stripping calculations, we note that for a given set of stripping and elastic-scattering data two questions should be answered: (1) Can the stripping data be fitted with acceptable parameters? (2) Are the stripping results sensitive to different choices of acceptable parameters? Depending on the results, several sets of conclusions may be drawn. For example, suppose that the answer is "yes" to (1) and "no" to (2). Then the calculations may be regarded as adequate and difficult improvements in the theory are not justified. The problem remains to establish why a theory which neglects so much is yet so successful. If the answer is "yes" to both (1) and (2), then the stripping calculations can be used to determine optical model parameters, but it would then be difficult to check improvements in the theory by comparing calculations with experiment. However, by including all features in the theory which one thinks are important, one's belief in the correctness of the optical-model parameter determinations would be strengthened. The answer of "no" to both (1) and (2) is the optimum case for improving the theory because one then need not worry about having the correct parameters but can proceed to test corrections to the theory by seeing whether their inclusion improves the agreement with experiment. Finally, if the answer is "no" to (1) and "yes" to (2), then it is possible that the correct parameter region has not been tried or that the data are in error. If neither is the case, the theory might be improved by adding effects to the theory and then trying a number of different parameter sets to determine whether a fit to the data does occur within the range of acceptable parameter sets.

In actual situations, one set of data may yield results that tend toward one extreme, whereas another set may yield results that tend toward another extreme. Thus by a judicious choice of data the investigator may suit his needs to a greater than average extent. In this regard he especially wants to reduce the dependence of the results on the choice of optical-model parameters.

In the following sections several nuclei for which suitable stripping and elastic-scattering data are available are considered in order to find regions of the parameter space which explain the elastic-scattering data; then various combinations of deuteron and proton parameter sets picked from different acceptable parameter regions are used to determine their effect on the stripping results. Due to the large number of possible parameter combinations and the difficulty in presenting an exhaustive treatment of all of them, the material included here should be regarded as merely representa-

tive. Thus, best-fit parameters from several entirely different regions of the parameter space are considered, and then various kinds of parameter deviations about one of the optimum sets are studied. Specific points of interest are whether or not the stripping data can be reasonably fitted, whether or not certain parameter regions can be eliminated from further consideration because of their yielding poor stripping results, and whether or not the stripping is sensitive to variations in the parameters.

### PROCEDURE

The pertinent facts about the stripping and elastic-scattering data used here are listed in Table I. The reactions are discussed in essentially the order in which they were investigated. The  $^{90}\text{Zr}(d,p)^{91}\text{Zr}$  reactions for  $E_d=10.85$  MeV were studied the most intensively, and the other reactions were then used to check and extend the zirconium results. This research employs a more efficient elastic-scattering parameter search routine<sup>20</sup> than that used in a similar study<sup>21</sup> of the  $^{90}\text{Zr}(d,p)^{91}\text{Zr}$  reaction. The previous work indicated that the  $l=0$ ,  $^{88}\text{Sr}(d,p)^{89}\text{Sr}$  stripping polarization is rather insensitive to the choice of elastic-scattering parameters, and therefore the polarization is not re-considered. A study somewhat similar to the one presented here was recently made<sup>18</sup> of the  $^{40}\text{Ca}(d,p)^{41}\text{Ca}$  reaction, in which the procedures used in making the calculations were varied, such as the inclusion of spin-orbit coupling and a finite-range neutron-proton potential, the use of parameters found from studying elastic data which show sizable fluctuations as a function of energy, and the consideration of potentials with different discrete real potential depths. Since the effects of using parameters from different acceptable regions of the parameter space were not extensively reported, the present work complements the  $^{40}\text{Ca}(d,p)^{41}\text{Ca}$  investigation.

Standard zero-range DWBA calculations are used here.<sup>13,22</sup> In particular, radial integrations extend to the origin, and shell-model wave functions for the neutron moving in a Woods-Saxon potential are used. The optical-model potentials for the deuteron and proton have the following form:

$$V = Vf(r) + iWg(r) - V_{s0} \left( \frac{\hbar^2}{m_n c^2} \right)^2 \frac{1}{r} \frac{d}{dr} f(r) + V_c, \quad (1)$$

where

$$f(r) = 1 / \{ 1 + \exp[(r-R)/a] \}, \quad (2)$$

$V_c$  = Coulomb potential due to a homogeneously charged

<sup>20</sup> R. N. Maddison, Proc. Phys. Soc. (London) **79**, 264 (1962); the author is indebted to F. G. Perey for pointing out the advantages of Maddison's method.

<sup>21</sup> W. R. Smith, Argonne National Laboratory Report No. ANL-6848, 1964 (unpublished).

<sup>22</sup> W. Tobocman, Phys. Rev. **94**, 1655 (1954).

TABLE I. List of reactions.

Reaction	$E$ (MeV)	$Q$ (MeV)	$l$	$j$	Reference
$^{90}\text{Zr}(d,p)^{91}\text{Zr}$	10.85	5.02	2	$\frac{5}{2}$	a
	15				b
	10.85	3.8	0	$\frac{1}{2}$	a
	15				b
	10.85	2.8	4	$\frac{7}{2}$	a
$\text{Zr}(d,d)\text{Zr}$	15				b
	11.8				c
	15				d
$\text{Nb}(p,p)\text{Nb}$	16.2				e
$^{91}\text{Zr}(p,p)^{91}\text{Zr}$	22.5				f
$^{52}\text{Cr}(d,p)^{53}\text{Cr}$	3.29	5.72	1	$\frac{3}{2}$	g
	4.07				
	5.72				h
	7.0				i
	7.0	5.15	1	$\frac{1}{2}$	
	7.0	4.72	3	$\frac{3}{2}$	
	7.0				i
	10.0				i
	10.13				h
	14.0	4.51	1	$\frac{1}{2}$	j
$^{206}\text{Pb}(d,p)^{207}\text{Pb}$	14.0				j
	14.0				k
	21.6				k
	17.0				l
	22.2				e
$\text{Zn}(d,p)^{65}\text{Zn}$	11.8	5.2	1	$\frac{1}{2}$	
			4	$\frac{3}{2}$	
			2	$\frac{5}{2}$	
$\text{Zn}(d,d)\text{Zn}$	11.8				c, m, n
$\text{Zn}(p,p)\text{Zn}$	17.0				o, p

<sup>a</sup> R. L. Preston, H. J. Martin, and M. B. Sampson, Phys. Rev. **121**, 1741 (1961).

<sup>b</sup> B. L. Cohen and O. V. Chubinsky, Phys. Rev. **131**, 2184 (1963).

<sup>c</sup> G. Igo, W. Lorenz, and U. Schmidt-Rohr, Phys. Rev. **124**, 832 (1961).

<sup>d</sup> See Ref. 27.

<sup>e</sup> C. B. Fulmer, Phys. Rev. **125**, 631 (1962).

<sup>f</sup> J. B. Ball, C. B. Fulmer, and R. H. Bassel, Phys. Rev. **135**, B706 (1964).

<sup>g</sup> I. Slaus, Nucl. Phys. **10**, 457 (1959).

<sup>h</sup> See Ref. 25.

<sup>i</sup> See Ref. 3.

<sup>j</sup> See Ref. 2.

<sup>k</sup> J. L. Yntema (private communication).

<sup>l</sup> G. Schrank and R. E. Pollock, Phys. Rev. **132**, 2200 (1963).

<sup>m</sup> See Ref. 7.

<sup>n</sup> See Ref. 8.

<sup>o</sup> I. E. Dayton and G. Schrank, Phys. Rev. **101**, 1358 (1956).

<sup>p</sup> See Ref. 6.

sphere of radius  $R$ , and  $R=R_0A^{1/3}$ . Three different choices of imaginary potential shapes are considered:

$$g_s(r) = 1 / \{ 1 + \exp[(r-R')/a'] \} \quad (\text{Woods-Saxon}), \quad (3)$$

$$g_d(r) = 4a \frac{d}{dr} g_s(r) \quad (\text{derivative}), \quad (4)$$

$$g_g(r) = 1 / \{ \exp[(r-R')/a']^2 \} \quad (\text{Gaussian}). \quad (5)$$

Also, the following conventions are adhered to:

$$(W)_n = 0, \quad \text{and} \quad (V_{s0})_n = 6 \text{ MeV}.$$

It should be stressed that, unless explicitly stated otherwise, the neutron potential has been constrained to have the same Woods-Saxon shape as the proton real potential; that is,

$$[f(r)]_n = [f(r)]_p.$$

The elastic-scattering best-fit criteria for  $N$  experi-

mental points is defined here as

$$X = \frac{100}{N} \left\{ \sum_{i=1}^N [(\sigma_{\text{ex}}(\theta_i) - \sigma_{\text{th}}(\theta_i)) / \sigma_{\text{ex}}(\theta_i)]^2 \right\}^{1/2}, \quad (6)$$

where  $\sigma_{\text{ex}}$  and  $\sigma_{\text{th}}$  are, respectively, the experimental and theoretical differential cross sections and  $\theta_i$  is the angular coordinate of the  $i$ th point. Sample elastic-scattering fits are shown in Fig. 1. A spin-orbit potential is included in the proton elastic-scattering calculations but not in the deuteron elastic-scattering calculations nor in the proton or deuteron channels of the stripping calculations. Thus the stripping calculations are made *without* a proton spin-orbit term; however, the proton parameters used were obtained from elastic-scattering calculations which *include* the spin-orbit interaction.

It has been shown<sup>7,8</sup> that for a suitable fixed radius

a series of discrete values of the deuteron real potential,  $V_d$ , give equally good fits to the elastic-scattering data. The use in stripping reactions of such discrete potentials has already been investigated<sup>3,18</sup> and will be given scant attention here. In this study the value of  $V_d$  used is the one which is roughly twice  $V_p$  when  $R_d = R_p$  and which best fits the stripping data.

The Nb( $p,p$ )Nb,  $^{52}\text{Cr}(d,d)^{52}\text{Cr}$ , and  $^{53}\text{Cr}(p,p)^{53}\text{Cr}$  absolute cross sections were not determined experimentally. To allow for this, the  $^{53}\text{Cr}(p,p)^{53}\text{Cr}$  data were normalized at small angles to some 9.76-MeV data for the elastic scattering of protons from natural chromium,<sup>23</sup> while the  $^{52}\text{Cr}(d,d)^{52}\text{Cr}$  data were left normalized as published since the resulting parameters yielded the best stripping fits when reasonable radii were used. However, the diffuseness ( $a_d$ ) obtained with this normalization appears anomalously small when compared with

TABLE II. Parameters<sup>a</sup> for  $^{90}\text{Zr}(d,p)^{91}\text{Zr}$ ,  $^{52}\text{Cr}(d,p)^{53}\text{Cr}$ ,  $^{206}\text{Pb}(d,p)^{207}\text{Pb}$ , and  $\text{Zn}(d,p)$  reactions.

	$R_0$	$a$	$R_0'$	$a'$	$V$	$W$	$V_{s0}$	$X$	Footnote
$^{90}\text{Zr}(d,p)^{91}\text{Zr}$									
$dA$	1.1*	0.7329	1.361	0.8692	104.8	10.02		0.5448	
$dB$	1.2*	0.6809	1.260	0.8634	92.12	12.2		0.469	
$dC$	1.282*	0.6234	1.160	0.8815	83.62	14.03		0.4516	
$dD$	1.287	0.6182	1.150	0.8885	83.20	14.08		0.4573	
$dE$	1.3*	0.6103	1.130	0.8926	81.91	14.39		0.4617	
$dF$	1.38*	0.5686	0.9746	0.9174	74.09	16.20		0.5770	
$dG$	1.38*	0.5608	1.084	0.337	74.88	55.51		0.5655	
$dH$	1.449	0.5062	1.062	0.3457	68.3	51.07		0.4542	
$dI$	1.282*	0.5996	1.547	0.8705	83.81	9.021		0.4691	b
$dJ$	1.282*	0.6292	0.9326	2.818	83.77	11.48		0.3999	c
$dK$	1.282*	0.6154	1.271	0.8871	83.62	12.65		0.4703	d
$dL$	1.2*	0.78*	1.35	0.7227	88.56	14.65		0.7743	
$dM$	1.2*	0.6228	1.41*	0.9137	90.59	8.544		0.5913	
$dN$	1.2*	0.7245	1.259	0.71*	92.51	16.34		0.6178	
$dO$	1.2*	0.59	1.106	1.011	97*	11.81		0.6948	
$dP$	1.2*	0.7076	1.219	0.7308	93.26	17.2*		0.6296	
$dQ$	1.2*	0.7171	1.28	0.8318	90.87	12.89		0.4367	e
$dR$	1.2*	0.6455	1.246	0.8909	93.3	11.5		0.6138	f
$dA'$	1.1*	0.8329	1.347	0.6638	103.9	15.44		1.645	
$dB'$	1.2*	0.7712	1.338	0.6082	90.71	18.26		1.753	
$DC'$	1.3*	0.3837	1.256	1.093	85.15	8.075		1.175	
$pA$	1.1*	0.6882	1.514	0.7628	61.94	5.295	8*	0.9251	
$pB$	1.2*	0.7161	1.257	0.5482	54.28	11.71	8*	0.8332	
$pC$	1.23*	0.7024	1.256	0.4605	52.02	14.49	8.518	0.8106	
$pD$	1.292	0.5504	0.9417	0.4382	48.66	17.84	8*	0.8141	
$pE$	1.3*	0.5521	0.9458	0.4375	47.94	17.63	8*	0.8164	
$pF$	1.23*	0.6191	1.414	0.2959	53.00	6.196	9.828	0.8664	b
$pG$	1.23*	0.6833	1.203	1.362	52.19	11.11	8.333	0.7969	c
$pH$	1.23*	0.6426	1.275	0.5335	52.48	8.549	9.353	0.8259	d
$pI$	1.2*	0.666*	1.218	0.6653	54.73	9.253	8*	0.8913	
$pJ$	1.2*	0.6312	1.16*	0.7051	55.45	9.1	8*	0.9927	
$pK$	1.2*	0.6952	1.258	0.65*	54.19	9.131	8*	0.8542	
$pL$	1.2*	0.7714	1.371	0.679	52*	7.863	8*	1.358	
$pM$	1.2*	0.695	1.265	0.6668	54.11	8.7*	8*	0.8614	
$pN$	1.2*	0.7523	1.27	0.5293	53.89	12.34	8*	1.015	e
$pO$	1.2*	0.6785	1.24	0.5701	54.75	11.14	8*	0.7061	f
$pA'$	1.1*	0.8986	1.34	0.5525	57.95	13.39	8*	2.022	
$pB'$	1.2*	0.7201	1.261	0.5781	51.47	10.92	8*	1.25	
$pC'$	1.3*	0.5585	1.219	0.5036	44.90	12.41	8*	1.863	

<sup>a</sup> Parameters marked with \* were not varied in the search. A derivative form was used for the imaginary potential except where noted otherwise.

<sup>b</sup> Woods-Saxon imaginary potential.

<sup>c</sup> Gaussian imaginary potential.

<sup>d</sup>  $\frac{1}{2}$  (derivative) plus  $\frac{1}{2}$  (Woods-Saxon) imaginary potential.

<sup>e</sup> Experimental angular distribution was renormalized by the factor 0.95.

<sup>f</sup> Experimental angular distribution was renormalized by the factor 1.05.

TABLE II.—Continued.

	$R_0$	$a$	$R_0'$	$a'$	$V$	$W$	$V_{s0}$	$X$	Footnote
$^{52}\text{Cr}(d,p)^{53}\text{Cr}$									
$dA$	1.15*	0.4509	1.39	0.9741	98.79	7.878		0.5277	
$dB$	1.2*	0.4243	1.36	0.9901	92.83	8.143		0.5206	
$dC$	1.3*	0.3616	1.277	1.039	82.97	8.712		0.5075	
$dD$	1.5*	0.6045	1.133	0.2344	61.26	91.03		0.5157	
$dE$	1.718	0.4118	1.139	0.2581	50.49	71.79		0.4579	
$pA$	1.15*	0.7789	1.353	0.6412	55.61	7.835	7.208	0.5014	
$pB$	1.2*	0.7452	1.32	0.5946	52.32	8.919	7.298	0.4334	
$pC$	1.3*	0.6577	1.278	0.4588	46.75	13.05	8.045	0.5030	
$pD$	1.3*	0.5761	0.8107	0.4443	48.00	15.38	5.701	0.4075	
$pA'$	1.2*	0.7342	1.301	0.5857	53.52	8.833	7.3*	1.384	
$^{206}\text{Pb}(d,p)^{207}\text{Pb}$									
$dA$	1.2*	0.2907	1.431	0.8899	114.1	2.616		0.6077	
$dB$	1.2*	0.5425	0.8512	1.15	108.9	10.35		0.8037	
$dC$	1.2*	0.3060	1.347	1.062	87.45	2.507		0.6538	
$dD$	1.25*	0.2699	1.342	1.041	106.4	2.823		0.7245	
$dE$	1.25*	0.5115	0.7385	1.251	101.1	11.23		0.9056	
$dA'$	1.2*	0.7843	1.269	0.7017	93.88	18.55		1.081	
$pA$	1.1*	0.5947	1.398	0.8635	70.87	4.202	7.818	0.7586	
$pB$	1.2*	0.4637	1.283	1.108	61.77	3.790	4.630	0.7949	
$pC$	1.25*	0.5080	1.062	1.294	56.05	5.138	0.8794	1.051	
$pA'$	1.2*	0.9094	1.395	0.9117	52.25	7.596	7.808	1.194	
$\text{Zn}(d,p)$									
$dA$	1.083	0.8350	1.354	0.7150	103.3	19.17			
$dB$	1.097	0.8510	1.371	0.7610	65.10	14.29			
$dC$	1.15	0.8100	1.340	0.6800	94.80	22.50			
$dD$	1.3	0.7300	1.340	0.6500	77.50	25.10			
$dE$	1.065	0.7900	1.720	0.6710	108.70	11.08			b
$pA$	1.25	0.6500	1.250	0.4700	48.50	12.40			
$pB$	1.318	0.6670	1.280	0.3640	44.52	18.37			
$pC$	1.104	0.7000	1.657	0.5610	59.13	5.280			b

values found for other nuclei.<sup>7</sup> The Nb( $p,p$ )Nb normalization was also left as given since the value yielded for the diffuseness ( $a_p$ ) was not far different from that determined by extensive searches for universal proton elastic-scattering parameters<sup>6</sup> ( $R_{0p} = 1.25 F$ ,  $a_p = 0.65 F$ ).

The parameters used in the discussion of the stripping results are listed in Table II in groups according to the target, the type of projectile (deuteron or proton), and the energy. Within a group the parameters are initially in the order of increasing  $R_0$ , next according to the various imaginary form factors used, then according to the parameter held constant in the search, and finally according to the normalization of the data.

For the extraction of spectroscopic factors the 10.85-MeV  $^{90}\text{Zr}(d,p)^{91}\text{Zr}$  results (shown later in Figs. 2–10) and the  $^{52}\text{Cr}(d,p)^{53}\text{Cr}$  results (shown later in Fig. 11) were first plotted together, in groups shown in the figures, so that if there were more than one curve in a group the curves deviated as little as possible from one another. Then each group was normalized as a whole to the data, with emphasis being placed on fitting the data at angles between approximately 20 and 100°. The  $l=4$ ,  $^{90}\text{Zr}(d,p)^{91}\text{Zr}$  data are not shown because they were obtained by an inaccurate method. The arbitrary value 1.4 mb/sr at 45° was used with the  $l=4$  calculations in the place of experimental data to obtain the spectroscopic factors. (Hence conclusions based on the

resulting absolute magnitudes of the spectroscopic factors would be meaningless.) For the other stripping reactions smooth curves were drawn through the data, and the scattering intensity was extracted at angles which are multiples of 5° and was then used to normalize the calculations by requiring that the sum over angles of the calculated intensity divided by the experimental intensity equal the number of angles. The angular range treated in this fashion was from 15 to 90° for the 15-MeV  $^{90}\text{Zr}(d,p)^{91}\text{Zr}$  data, from 15 to 80° for the  $^{52}\text{Cr}(d,p)^{53}\text{Cr}$  angular distributions, from 10 to 155° for  $^{206}\text{Pb}(d,p)^{207}\text{Pb}$ , and 5 to 90° for the Zn( $d,p$ ) reactions. For the latter case experimental data were not used. Instead, the calculations were normalized to a particular one of the calculated results.

The spectroscopic factors are defined here as the factors that the calculated differential cross sections must be multiplied by to get the relative normalizations between calculation and experiment described above. In the notation used here,  $S_l$  represents the spectroscopic factor corresponding to the reaction with neutron capture angular momentum  $l$ , and  $S_{lk}$  is defined as  $S_l/S_k$ . Furthermore,  $S_l'$  represents  $S_l$  divided by some particular  $S_k$  to be specified as needed, and  $S_{lk}' = S_l'/S_k'$ . In Tables III and IV the linear averages of groups of spectroscopic factors are given, and also shown are the percentage deviations from the averages

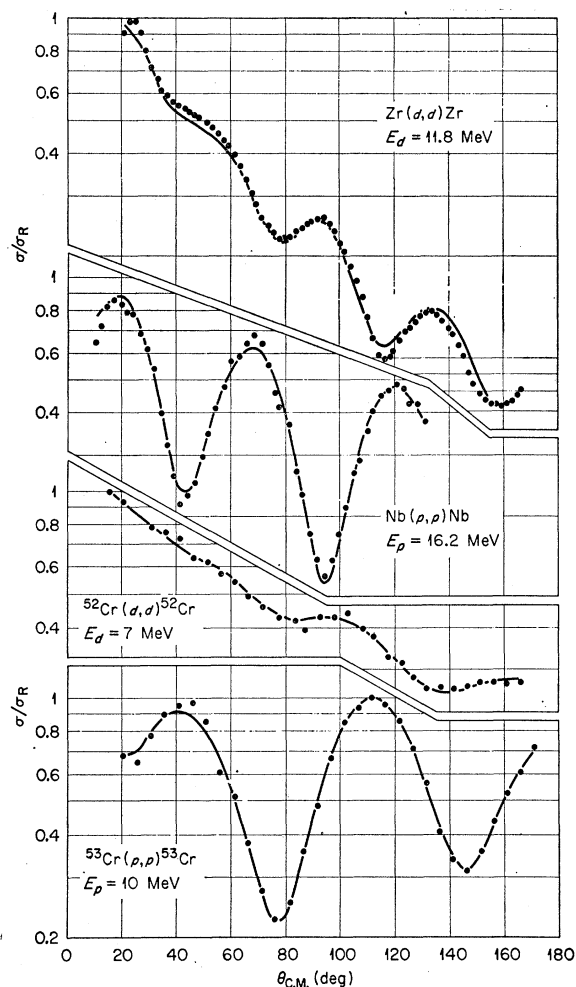


FIG. 1. Optical-model calculations compared with experimental proton and deuteron elastic-scattering angular distributions. The parameters used are listed in Table II as  $^{90}\text{Zr}(d,p)^{91}\text{Zr}$  sets  $dB$  and  $pB$  and  $^{52}\text{Cr}(d,p)^{53}\text{Cr}$  sets  $dB$  and  $pB$ .

defined as

$$100|S_i - (S_i)_{\text{av}}| / (S_i)_{\text{av}}$$

Table IV also gives deviations, percent  $D_o$ , of the

spectroscopic factors from those spectroscopic factors calculated with the central set of parameters about which parameter variations were carried out.

One final matter: The deuteron internal wave function is assumed here to be normalized as if the  $(n,p)$  interaction had zero range. If the normalization were chosen to correspond to the use of a finite-range Hulthén potential, then the spectroscopic factors listed here would have to be reduced by a factor of  $\frac{2}{3}$ .<sup>24</sup>

## RESULTS

### $^{90}\text{Zr}(d,p)^{91}\text{Zr}$

Figures 2–5 show the results of studies with parameters from different regions of the parameter space. Figures 6–10 give the results corresponding to parameter variations about a central set of parameters. The latter idea is that, since some errors are most likely involved in the data, somewhat inferior fits cannot be ruled out as unsuitable. Allowing other than optimum fits greatly extends the range of suitable parameters, and obviously the region cannot be exhaustively investigated. So instead I displaced one parameter at a time far enough for it to be significantly different from its central value, but not so far that the quality of fit obtained when all the other parameters were readjusted for the best fit was seriously impaired. This method should give some indication of whether or not the stripping shows any appreciable changes when the parameters are allowed to vary throughout the valley of acceptable fits, and thus whether different data would be expected to yield significantly different results if again only the optimum parameters were allowed.

An extensive search was made in the case of  $\text{Zr}(d,d)\text{Zr}$  to find different absolute minima in the parameter space. By “absolute” minima is meant that no set of parameters in the vicinity of the minima (vicinity could be taken to mean roughly within the perimeter of 10% variation of each parameter) yields as low a value of  $X$ . Only two were found, these being significantly different in the values of  $R_0$ ,  $a'$ , and  $W$ . Since, as will be shown later, the results are sensitive to  $R_0$ , an intermediate  $R_0$  was chosen and the values of  $a'$

TABLE III.  $S_i$  values for Figs. 4 and 5.

	$S_0$	Percent deviation	$S_2$	Percent deviation	$S_4$	Percent deviation	$S_0/S_2$	Percent deviation	$S_4/S_2$	Percent deviation
Deuteron imaginary potential										
Derivative	0.425	0.7	0.614	1.5	0.392	0.3	0.693	2.4	0.639	1.4
W-S	0.425	0.7	0.631	1.2	0.405	3.1	0.673	0.5	0.641	1.8
Gaussian	0.403	4.5	0.618	0.9	0.375	4.6	0.653	3.5	0.607	3.7
Derivative+W-S	0.434	2.8	0.631	1.2	0.400	1.8	0.687	1.6	0.634	0.6
Average	0.422	2.2	0.624	1.2	0.393	2.4	0.677	2.0	0.630	1.9
Proton imaginary potential										
Derivative	0.425	8.4	0.582	9.7	0.392	8.5	0.730	1.3	0.674	1.3
W-S	0.500	7.6	0.702	8.9	0.455	6.2	0.711	1.3	0.648	2.6
Gaussian	0.448	3.5	0.615	4.6	0.416	2.9	0.728	1.0	0.676	1.6
Derivative+W-S	0.484	4.3	0.679	5.4	0.451	5.3	0.713	1.0	0.664	0.2
Average	0.464	6.0	0.645	7.1	0.429	5.7	0.721	1.1	0.666	1.4

<sup>24</sup> R. H. Bassel, R. M. Drisko, and G. R. Satchler, Oak Ridge National Laboratory Report No. ORNL-3240, 1962 (unpublished).

TABLE IV.  $S_i$  values for Figs. 6, 7, 8, and 9.<sup>a</sup>

	$S_0$	Percent deviation $D_e$	$S_2$	Percent deviation $D_e$	$S_4$	Percent deviation $D_e$	$S_0/S_2$	Percent deviation $D_e$	$S_4/S_2$	Percent deviation $D_e$
$R_{0p}=1.1$ F;	0.995	24.6	1.227	23.5	1.070	40.2	0.811	2.7	0.872	20.3
$R_{0d}=1.1$ F				68.0				16.2		36.2
$R_{0p}=1.3$ F;	0.509	36.2	0.701	29.5	0.425	44.3	0.725	8.2	0.606	16.4
$R_{0d}=1.3$ F				3.9				3.2		5.3
$R_{0p}=1.1$ F;	1.080	35.3	1.237	24.5	1.180	54.7	0.874	10.6	0.955	31.7
$R_{0d}=1.3$ F				69.5				25.7		49.2
$R_{0p}=1.3$ F;	0.608	23.8	0.809	18.6	0.376	50.7	0.751	4.9	0.465	35.8
$R_{0d}=1.1$ F				10.8				7.1		27.4
Average	0.798	30.0	0.994	24.0	0.763	47.5	0.790	6.6	0.725	26.1
$\Delta a_d = 0.1$ F	0.556	8.8	0.760	2.4	0.471	2.4	0.732	6.3	0.619	0
$\Delta V_d = 5$ MeV	0.528	3.3	0.800	7.8	0.475	3.3	0.660	4.2	0.594	4.0
$\Delta W_d = 5$ MeV	0.501	2.0	0.711	4.2	0.418	9.1	0.705	2.3	0.587	5.2
$\Delta R_{0d}' = 0.15$ F	0.497	2.7	0.745	0.4	0.514	11.7	0.667	3.2	0.689	11.3
$\Delta a_d' = -0.15$ F	0.473	7.4	0.695	6.3	0.422	8.3	0.680	1.3	0.607	1.9
Average	0.511	4.8	0.742	4.2	0.460	7.0	0.689	3.5	0.619	4.5
$\Delta a_p = -0.05$ F	0.557	1.8	0.809	0.6	0.553	1.7	0.690	2.4	0.684	2.2
$\Delta V_p = -2.3$ MeV	0.582	6.5	0.841	3.5	0.539	0.8	0.692	2.7	0.640	4.3
$\Delta W_p = -3$ MeV	0.523	4.5	0.788	3.1	0.531	2.3	0.664	1.5	0.674	0.7
$\Delta R_{0p}' = -0.1$ F	0.543	0.8	0.829	2.0	0.558	2.7	0.655	2.8	0.673	0.6
$\Delta a_p' = 0.1$ F	0.532	2.8	0.797	1.9	0.537	1.2	0.667	1.0	0.673	0.6
Average	0.5474	3.3	0.8128	2.2	0.5436	1.8	0.674	2.1	0.669	1.7
$F_p = 0.95$ ;	0.521	0.8	0.716	4.7	0.436	6.0	0.727	3.9	0.609	1.5
$F_d = 0.95$				3.1				0.6		2.2
$F_p = 1.05$ ;	0.559	6.5	0.782	4.1	0.497	7.1	0.715	2.1	0.635	2.7
$F_d = 0.95$				5.8				1.1		1.9
$F_p = 0.95$ ;	0.492	6.3	0.730	2.8	0.439	5.4	0.674	3.7	0.601	2.7
$F_d = 1.05$				1.2				6.8		3.5
$F_p = 1.05$ ;	0.529	0.8	0.775	3.2	0.485	4.5	0.682	2.6	0.626	1.3
$F_d = 1.05$				4.9				5.7		0.5
Average	0.525	3.6	0.751	3.7	0.464	5.8	0.700	3.1	0.618	2.1
				3.8				3.5		2.1

<sup>a</sup>  $D_e$  = deviation from the results obtained using a central set of parameters.

and  $W$  were biased so that in the ensuing search the parameter sets yielded would correspond to the two types found previously. In Fig. 2 the parameters with the smaller  $R_0$  yield a slightly better fit to the data, although the data for the  $l=0$  case are not of sufficient accuracy for a firm decision to be made between the two. In Fig. 3, making  $R_0$  the same for both cases causes the differences to diminish in the  $l=0$  and 2 cases. Setting the radii equal is seen to have little effect on making the  $S_l$  more alike.

In Figs. 4 and 5 the results of using different analytic forms for the imaginary potentials are compared. Four types are considered: two surface-peaked forms, a Woods-Saxon volume type, and a mixture of volume and surface forms. The same radius was used for each after searches with all the parameters varied yielded similar radii in each case. The derivative shape for the proton imaginary potential produces angular distributions which differ somewhat from those given by the other three types. Otherwise the angular distributions are almost identical. The differences in the spectroscopic factors are quite moderate compared with those produced by some other types of parameter ambiguities.

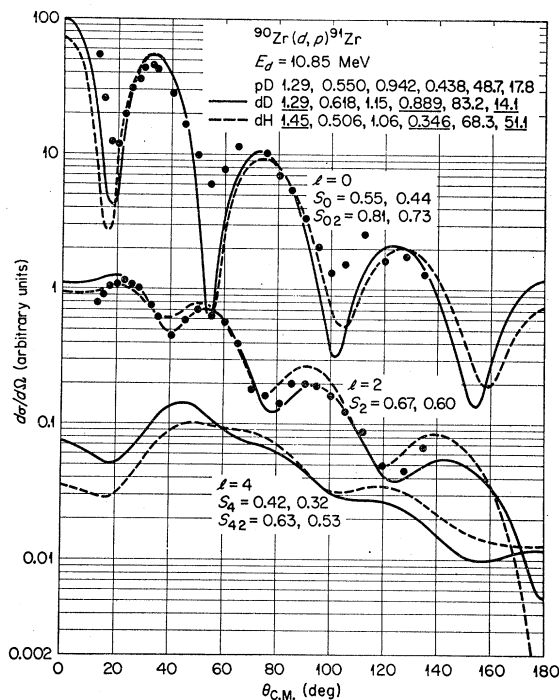


FIG. 2. Calculations of  $^{90}\text{Zr}(d,p)^{91}\text{Zr}$  angular distributions using deuteron parameter sets which are the optimum in two different regions of the parameter space. The proton and deuteron optical-model parameters are listed at the top of the figure in the order (left to right)  $R_0$ ,  $a$ ,  $R_0'$ ,  $a'$ ,  $V$ , and  $W$ . The parameters are also listed in Table II and correspond there to sets pD, dD, and dH. In addition, the corresponding spectroscopic factors  $S_l$  are shown on the figure, along with the ratios  $S_{l2} = S_l/S_2$ . The left-to-right order of the  $S_l$ 's and  $S_{l2}$ 's corresponds to the top-to-bottom order of the different parameter sets specified on the figure (in this case the two deuteron parameter sets). The experimental data corresponding to the  $l=0$  and 2 transitions are also shown.

Figure 6 shows the effects of fixing the proton and deuteron radius  $R_0$  at different values and optimizing the other parameters. The effects on both the angular distributions and the  $S_l$  are seen to be appreciable. Varying the proton (or neutron) radius is seen to have a larger effect on the spectroscopic factors than does varying the deuteron radius.

Since the neutron well was constrained to be identical to the proton well, additional calculations were made in which (1) the proton well was held fixed, and first the neutron radius and then the neutron diffuseness was varied, and (2) the neutron well was kept constant and the proton radius was changed. (The other parameters were varied so as to maintain the fit to the elastic-scattering data.) The resulting spectroscopic factors are listed in Table V. The  $S_l$  are seen to decrease significantly when either  $R_{0n}$ ,  $a_n$ , or  $R_{0p}$  is increased. Furthermore, changing  $R_{0n}$  from 1.1 to 1.3 F has almost identically the same effect on the angular distributions (not shown) as varying  $a_n$  from 0.4 to 1.0 F. Going from  $R_{0p} = 1.1$  F to  $R_{0p} = 1.3$  F does not cause the same type of effect in the angular distributions, but does produce the same amount of variation, as a similar change in  $R_{0n}$ . These results imply that as much attention should be given to finding the correct neutron potential parameters as is spent on determining the proton parameters.

The effects of increasing either  $R_{0n}$  or  $a_n$  can easily be understood when it is realized that such extensions of the neutron potential serve to decrease the size of

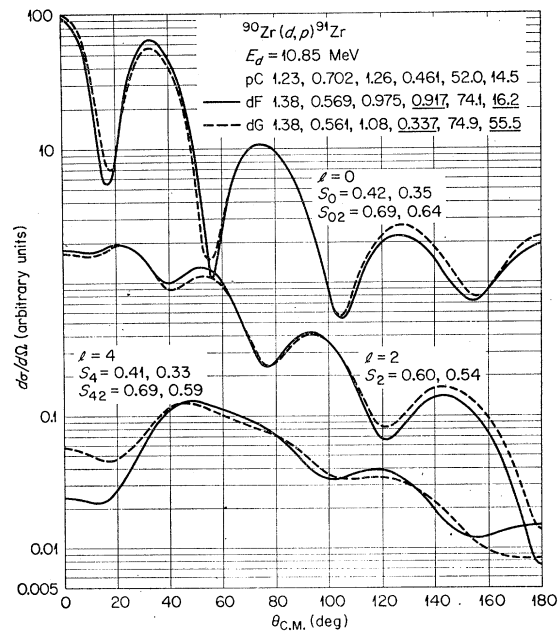


FIG. 3. Same as Fig. 2 except that the deuteron radius  $R_0$  was fixed at an intermediate value and the other parameters were then optimized after being initially biased to correspond to the two distinct regions of parameter space investigated in Fig. 2. The parameters correspond to sets pC, dF, and dG of Table II.

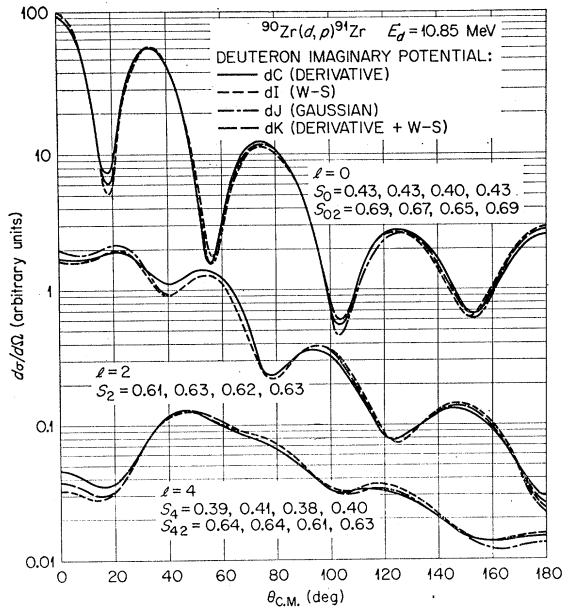


FIG. 4. Calculations using different types of deuteron imaginary potential form factors. Parameter sets  $\rho C$ ,  $dC$ ,  $dI$ ,  $dJ$ , and  $dK$  of Table II have been employed and the spectroscopic factors are given in Table III.

the interior oscillations of the radial wave function relative to the exterior values. This effect would thus reduce the interior contributions to the radial stripping integrals in a manner similar to that obtained by using a finite-range ( $n, p$ ) interaction, nonlocal potentials, or large deuteron or proton absorption potentials. Since a large portion of the stripping occurs in the surface of the target, the main effect of a neutron wave function damped in the interior would show up when the wave function is normalized throughout space; namely, there would be an increase in the calculated stripping cross section (i.e., a decrease in  $S_i$ ).

To explore parameter regions which give elastic-scattering fits somewhat less than optimum, parameter searches for  $Zr(d, d)Zr$  and  $Nb(p, p)Nb$  were made,

TABLE V.  $S_i'$  values for 10.85-MeV  $^{90}Zr(d, p)^{91}Zr$  neutron potential variations.<sup>a</sup>

	$S_0'$	$S_2'$	$S_4'$	$S_0'/S_2'$	$S_4'/S_2'$
$R_{0n} = 1.1$ F	1.29	1.27	1.62	1.02	1.28
$= 1.3$ F	0.73	0.75	0.61	0.97	0.80
Ratio (1.1/1.3)	1.77	1.69	2.68	1.05	1.59
$a_n = 0.4$ F	1.78	1.51	1.68	1.18	1.11
$= 1.0$ F	0.53	0.61	0.52	0.87	0.86
Ratio (0.4/1.0)	3.34	2.47	3.24	1.35	1.30
$R_{0p} = 1.1$ F	1.56	1.24	1.43	1.26	1.15
$= 1.3$ F	1.13	1.02	0.97	1.11	0.96
Ratio (1.1/1.3)	1.39	1.22	1.47	1.14	1.20

<sup>a</sup> The calculations are normalized to the angular distribution obtained by using parameter sets  $dB$  for the deuteron and  $pB$  for the proton and neutron. The angular range was 20–100°. Other than when varied, the neutron parameters are  $R_{0n} = 1.2$  F and  $a_n = 0.7161$  F. Parameter sets  $dB$  and  $pB$  are used, except that sets  $pA$  and  $pE$  are employed when  $R_{0p} = 1.1$  and 1.3 F, respectively.

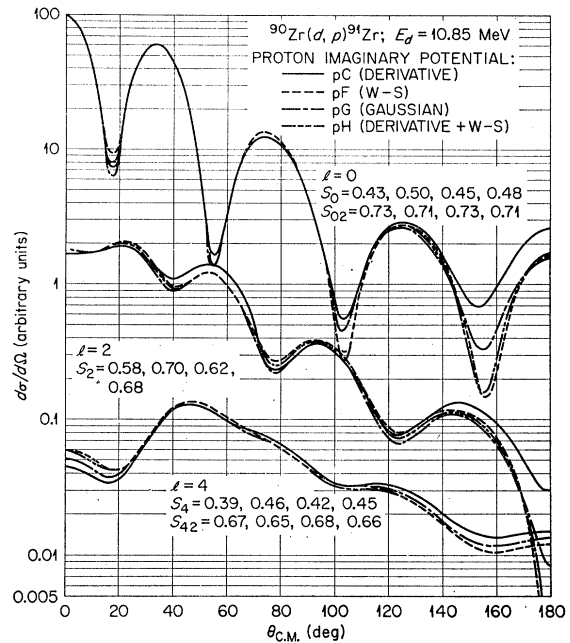


FIG. 5. Same as Fig. 4 except that different types of proton imaginary potential form factors have been used. Parameter sets  $\rho C$ ,  $pF$ ,  $pG$ ,  $pH$ , and  $dC$  of Table II have been employed.

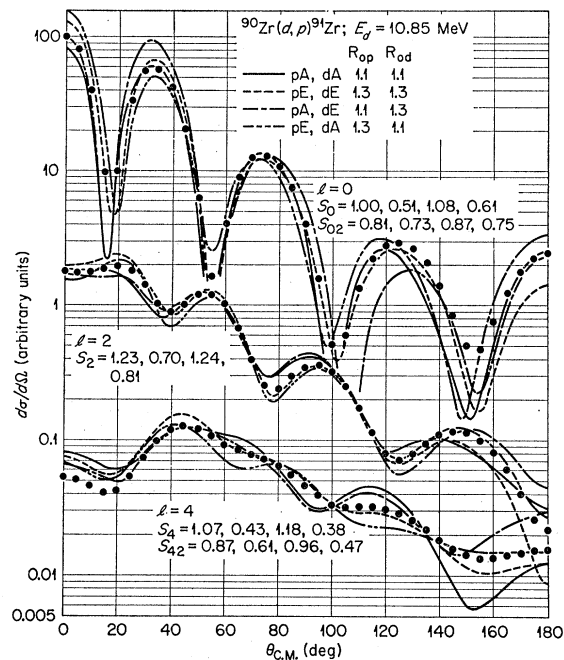


FIG. 6. Results of  $^{90}Zr(d, p)^{91}Zr$  calculations in which  $R_{0p}$  and  $R_{0d}$  were displaced from the intermediate value 1.2 F and held fixed while the other parameters were varied to optimize the fits to the elastic-scattering data. The closed circles are not experimental data but correspond to calculations made with the optimum parameter sets listed in Table II as sets  $pB$  and  $dB$ , and which yield the elastic-scattering results shown in Fig. 1. The parameters are sets  $pA$ ,  $pE$ ,  $dA$ , and  $dE$  of Table II and the spectroscopic factors are listed in Table IV.

starting with parameter sets  $dB$  and  $pB$  of Table II, then displacing one other parameter and holding it, together with  $R_0$  and  $V_{s0}$ , constant, and finally varying the other parameters so as to minimize  $X$ . The amount each parameter was displaced was adjusted to keep  $X$  from becoming too large. Comparing parameter sets  $dL$ ,  $dM$ ,  $dN$ ,  $dO$ , and  $dP$  with the central set  $dB$  and comparing sets  $pI$ ,  $pJ$ ,  $pK$ ,  $pL$ , and  $pM$  with the central set  $pB$  shows that the deuteron parameters are less critically determined by the data, particularly  $V_d$ , than are the proton parameters—undoubtedly because deuteron angular distribution does not exhibit such well-defined peaks and minima as does the proton data. Figure 8 shows that, except for the set wherein  $V_p$  is displaced (the corresponding value of  $X$  is anomalously large, anyway), the various proton potentials give essentially the same angular distributions. By comparison, Fig. 7 shows that variations in the deuteron parameters cause somewhat greater differences among the stripping angular distributions than do variations in the proton parameters. The situation is reversed for the spectroscopic factors. The important quantity in Table IV is percent  $D_e$ , the percentage deviation of the spectroscopic factors from the values found by using the central set of parameters. These are seen to be approximately 10% for the proton parameters but less than 5% for the deuteron parameters. It is noteworthy that the deviations in the relative spectroscopic factors are of moderate size when the

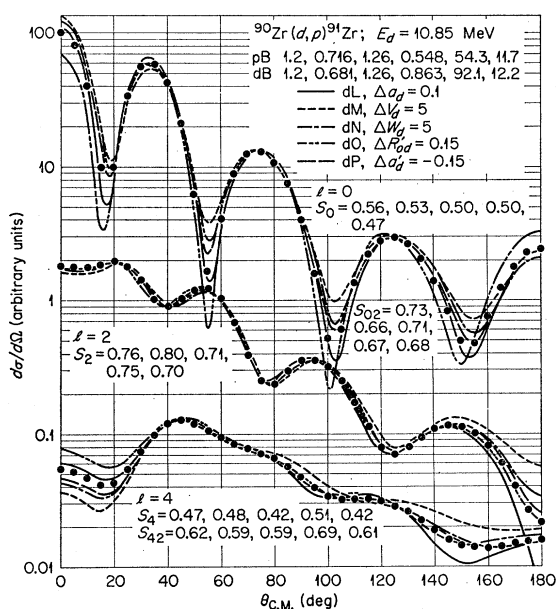


FIG. 7. Similar to Fig. 6 except that the proton parameters and  $R_{0d}$  have been held fixed, whereas each of the remaining parameters has been displaced one at a time from its value in the optimum set (listed at the top of the figure) and the other parameters have been varied to obtain the best agreement with the elastic-scattering data. The parameters are sets  $pB$ ,  $dL$ ,  $dM$ ,  $dN$ ,  $dO$ , and  $dP$  of Table II.

absolute  $S_l$  differences are large. Other than this, the variations in the  $S_l$  and  $S_1/S_2$  appear to be of random size. This apparent randomness may in part reflect the arbitrariness present in the method chosen for normalizing the calculations to experiment.

It is significant that, although the values of  $X$  corresponding to the displacements of  $R_{0d}$  and  $R_{0p}$  used in obtaining the results shown in Fig. 6 are on the average less than those corresponding to the parameter sets used in the calculations shown in Figs. 7 and 8, the differences generated in the angular distributions and spectroscopic factors are much larger in the former case than in the latter.

To investigate the dependence of the stripping results on errors in the absolute cross section of the

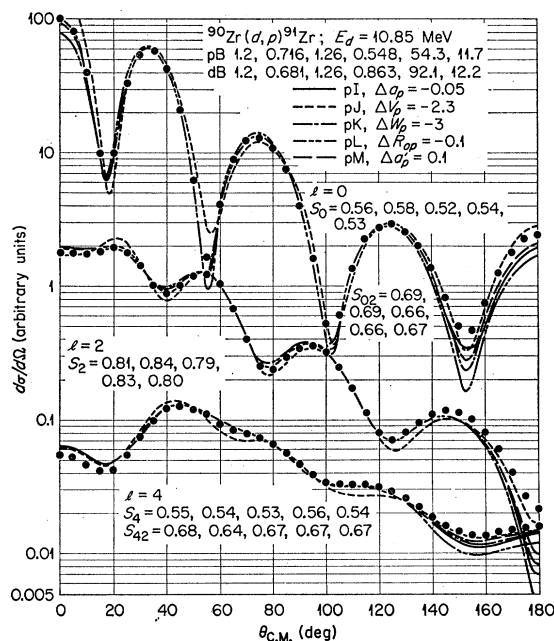


FIG. 8. Same as Fig. 7 except that the effects of individual variations in the proton parameters have been investigated. The parameters are sets  $pI$ ,  $pJ$ ,  $pK$ ,  $pL$ ,  $pM$ , and  $dB$  of Table II.

elastic scattering, the normalization of the experimental elastic-scattering angular distributions was varied by  $\pm 5\%$ , and (holding  $R_0$  and  $V_{s0}$  constant) the parameter sets were found which minimized  $X$ . Judging from the stripping angular distributions in Fig. 9 and the corresponding spectroscopic factors in Table IV, 10% errors in the absolute-cross-section determination are not serious for stripping calculations.

The preceding results involved 10.85-MeV  $^{90}\text{Zr}(d,p)^{91}\text{Zr}$ , 11.8-MeV  $\text{Zr}(d,d)\text{Zr}$ , and 16.2-MeV  $\text{Nb}(p,p)\text{Nb}$  data. For comparison purposes, calculations with 15-MeV  $^{90}\text{Zr}(d,p)^{91}\text{Zr}$  data, based on parameters obtained from the study of 15-MeV  $\text{Zr}(d,d)\text{Zr}$  and 22.5-MeV  $^{91}\text{Zr}(p,p)^{91}\text{Zr}$  data, were made in which the effects of varying  $R_{0d}$  and  $R_{0p}$  were studied. The results are

shown in Fig. 10 and correspond in method to the 10.85-MeV  $^{90}\text{Zr}(d,p)^{91}\text{Zr}$  results shown in Fig. 6. Again there is seen a noticeable dependence of both the spectroscopic factors and the angular distributions on the choice of radii. Three discrepancies between the different energy stripping results stand out: for the  $l=0$  and 2 cases for which 10.85-MeV ( $d,p$ ) data are available, the 15-MeV  $S_l$  average is roughly one-and-a-half times as large as for 10.85 MeV; the variations in the  $S_l$  at 15 MeV are not as large as they are at 10.85 MeV; and whereas the relative variations of the  $S_l$  and  $S_{l2}$  are similar for both energies in the  $l=2$  and 4 cases, they differ in the  $l=0$  case and, indeed, the  $S_0$  at  $E_d=15$  MeV show a strong dependence on the deuteron radius and not on the proton radius as in the 10.85-MeV results. These calculations indicate that it is advisable, when possible, to check the reliability of spectroscopic factor determinations by considering data at more than one energy.

Also interesting is a comparison of the elastic-scattering parameters obtained at the different energies. The 22.5-MeV proton parameter sets  $pA'$ ,  $pB'$ , and  $pC'$  may be compared with the 16.2-MeV sets  $pA$ ,  $pB$ , and  $pE$ ; and the 15-MeV deuteron sets  $dA'$ ,  $dB'$ , and  $dC'$  may be compared with the 11.8-MeV sets  $dA$ ,  $dB$ , and  $dE$ . Sets  $pB$  and  $pB'$  are closely alike; in fact, by using the radius  $R_{0p}=1.2$  F, the 22.5-MeV data can be fitted quite well by varying only  $V_p$  from the value obtained in the 16.2-MeV study. The same statements cannot be made regarding the other two

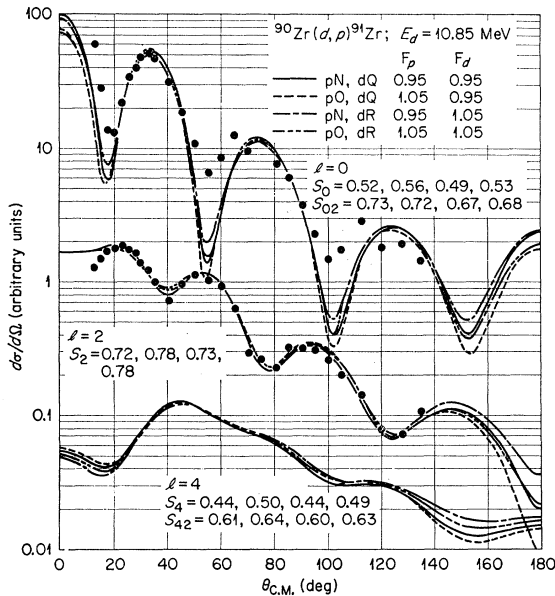


FIG. 9.  $^{90}\text{Zr}(d,p)^{91}\text{Zr}$  calculations using parameters obtained by fitting the experimental proton and deuteron elastic-scattering angular distributions after they had each been changed in absolute magnitude, first by a factor of 0.95 and then by 1.05. The parameter sets obtained in this way are sets  $pN$ ,  $pO$ ,  $dQ$ , and  $dR$  in Table II. The experimental data corresponding to the  $l=0$  and 2 transitions are shown on the figure.

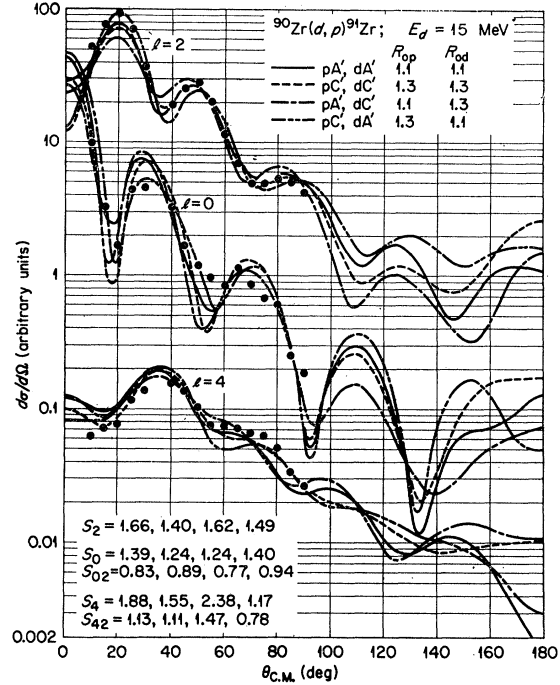


FIG. 10. Comparison between theory and experiment for  $E_d=15$  MeV,  $^{90}\text{Zr}(d,p)^{91}\text{Zr}$  reactions in which various combinations of deuteron and proton potential radii have been employed. The parameters are sets  $dA'$ ,  $dC'$ ,  $pA'$ , and  $pC'$  in Table II.

choices of radii studied. Thus, consideration of different-energy data indicates that the range of acceptable proton radii can be narrowed. The deuteron parameter sets for the two energies differ in detail; however, comparison of sets  $dQ$  and  $dR$ —wherein the absolute cross section of the 11.8-MeV data has been varied— with set  $dB'$  indicates that if the normalization of the 11.8-MeV data were changed by a factor of about 0.9 the agreement between the parameters at the two energies would be improved.

In Table VI the effects on the  $S_l$  of allowing the proton parameters to be varied independently of the neutron parameters, and vice versa, are presented. The parameters are initially fixed to sets  $dB'$  and  $pB'$ ; then

TABLE VI.  $S_l$  values for 15-MeV  $^{90}\text{Zr}(d,p)^{91}\text{Zr}$  neutron potential variations.<sup>a</sup>

	$S_0$	$S_2$	$S_4$	$S_0/S_2$	$S_4/S_2$
$R_{0n}=1.1$ F	1.10	1.23	1.47	0.89	1.19
$=1.3$ F	1.28	1.30	1.21	0.98	0.94
Ratio (1.1/1.3)	0.86	0.95	1.21	0.91	1.27
$R_{0p}=1.1$ F	1.37	1.54	1.74	0.81	1.13
$=1.3$ F	1.18	1.25	1.34	0.94	1.06
Ratio (1.1/1.3)	1.17	1.23	1.31	0.87	1.06

<sup>a</sup> The calculations are normalized to a smooth average of the experimental data between the angles of 15 and 90°. Parameter sets  $dB'$  and  $pB'$  are used, except that changes in the proton, or neutron, radius correspond to use of the appropriate parameter sets  $pA'$  or  $pC'$ . More explicitly, when the proton radius is changed, the neutron parameters are kept fixed at the  $pB'$  parameter values and vice versa.

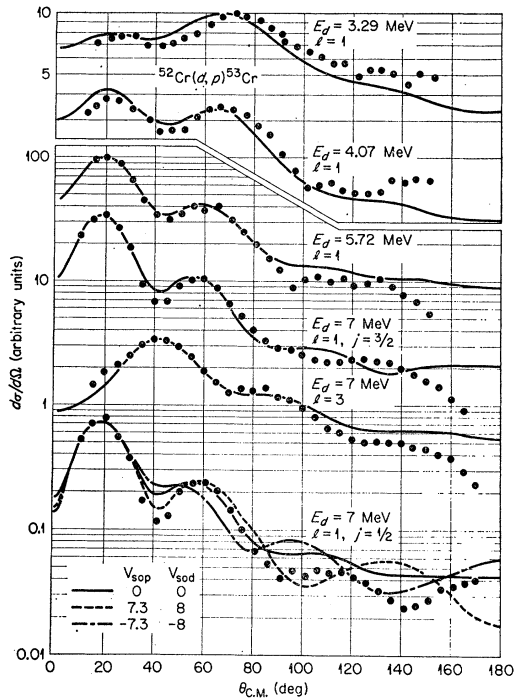


FIG. 11. Calculations of  $^{52}\text{Cr}(d,p)^{53}\text{Cr}$  angular distributions compared with experiment. Calculations for the  $l=1$ ,  $j=\frac{3}{2}$  transition are shown with no spin-orbit coupling and with positive and negative spin-orbit coupling in the proton and deuteron channels. The parameter sets used are listed as sets  $pB$  and  $dB$  in Table II.

first the neutron and then the proton parameters are chosen to be parameter sets  $pA'$  and  $pC'$ . This method differs from the 10.85-MeV method of Table VI in that  $R_{0n}$  and  $a_n$  are not varied separately. Since  $a_p$  (and hence  $a_n$ ) decreases as  $R_{0p}$  (and hence  $R_{0n}$ ) increases and since Table VI shows that increasing either  $R_{0n}$  or  $a_n$  reduces the  $S_l$  values, the increase in  $R_{0n}$  and the decrease in  $a_n$  counteract each other in their effect on the  $S_l$ . There is a significantly larger difference between the  $a_p$  for the two radii  $R_{0p}=1.1$  and  $1.3$  F at  $E_d=15$  MeV than between the  $a_p$  at  $E_d=10.85$  MeV. This larger difference is of such a nature as to cause a lesser variation of the  $S_l$  at 15 MeV than at 10.85 MeV. Furthermore, at  $E_d=15$  MeV the effect of the cancellation is more complete for the  $l=0$  case than for the  $l=4$  case.

### $^{52}\text{Cr}(d,p)^{53}\text{Cr}$

A single set of parameters (sets  $dB$  and  $pB$  of Table II) was used to obtain fits corresponding to the  $l=1$ ,  $^{52}\text{Cr}(d,p)^{53}\text{Cr}$  ground-state transition at energies of 3.29, 4.07, 5.72, and 7 MeV. As seen in Fig. 11, these calculations reproduce quite well the energy-dependent changes of the experimental angular distributions—even at energies well below the Coulomb barrier. The same parameters also fit the  $l=3$ ,  $^{52}\text{Cr}(d,p)^{53}\text{Cr}$  transition to the second excited state for  $E_d=7$  MeV, and

at the same time yield the agreement shown in Fig. 1 with the 7-MeV  $^{52}\text{Cr}(d,d)^{52}\text{Cr}$  and 10-MeV  $^{53}\text{Cr}(p,p)^{53}\text{Cr}$  data. Proton parameter set  $pA'$ , obtained from fitting 10.13-MeV  $^{53}\text{Cr}(p,p)^{53}\text{Cr}$  data,<sup>25</sup> checks the determination of parameter set  $pB$ . On the other hand, since the experimental deuteron elastic data are unnormalized, there is no assurance that the deuteron parameter set  $dB$  actually corresponds to that which would be predicted by a known correct set of deuteron elastic-scattering data. The diffuseness  $a_d$  is anomalously small [compare with the  $\text{Zr}(d,d)\text{Zr}$  parameters]; however, for the radius  $R_{0d}=1.2$  F neither the elastic scattering nor the stripping is fitted as well when a smaller normalization—yielding a larger  $a_d$ —is chosen.

At the bottom of Fig. 11 are shown the results of calculations for the  $l=1$ ,  $^{52}\text{Cr}(d,p)^{53}\text{Cr}$  transition to the first excited state which include spin-orbit coupling in both the proton and the deuteron channels. The sign convention used is such that a positive potential gives the correct sign for the proton elastic-scattering polarization. The use of positive spin-orbit potentials improves the agreement with experiment at angles between 30 and 110°, whereas the use of negative  $V_{s0}$  yields better agreement at larger angles. Thus, inclusion of the spin-orbit potentials, while not yielding over-all good fits, changes the angular distributions in approximately the right places and by the correct magnitudes to account for the discrepancies in the fits; so it seems likely that some form of spin-orbit or tensor interaction is appropriate, although not the one used here.

It was hoped that introduction of the energy dependence of the  $V_p$  and  $V_d$  suggested by Perey<sup>6,7</sup> into the calculations would improve the  $^{52}\text{Cr}(d,p)^{53}\text{Cr}$  fits at low energies. The low-energy fits were indeed im-

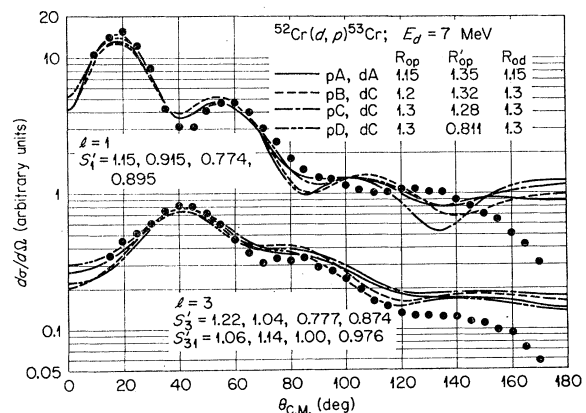


FIG. 12.  $^{52}\text{Cr}(d,p)^{53}\text{Cr}$  calculations which show satisfactory agreement with the experimental stripping data and at the same time use parameters which yield good agreement with the elastic-scattering data. The parameters are sets  $pA$ ,  $pB$ ,  $pC$ ,  $pD$ ,  $dA$ , and  $dC$  of Table II.

<sup>25</sup> J. C. Legg, H. D. Scott, and M. K. Mehta, Argonne National Laboratory Report No. ANL-6848, 1964 (unpublished).

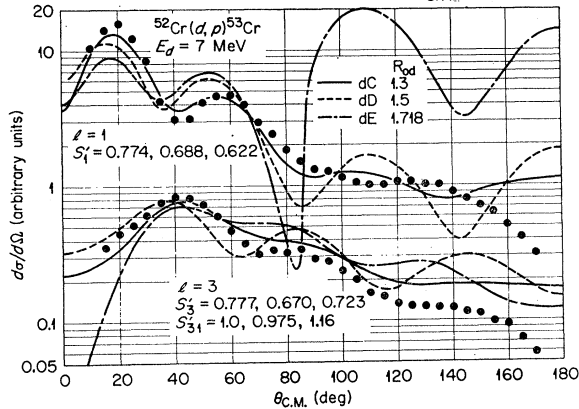


FIG. 13.  $^{52}\text{Cr}(d,p)^{53}\text{Cr}$  calculations which correspond to parameter sets using different values of  $R_{0d}$  and which yield good agreement with the deuteron elastic-scattering data. Parameter sets  $pC$ ,  $dC$ ,  $dD$ , and  $dE$  of Table II have been employed.

proved slightly, but at the expense of slightly worse fits to the 7-MeV data. The differences in results are small, however, and larger changes in  $V_p$  and  $V_d$  appear to be necessary.

Proton parameter sets  $pA$ ,  $pB$ , and  $pC$  cover the flat bottom portion of the  $VR^n$  ambiguity for one type of potential, and  $pD$  corresponds to another type of potential having a smaller  $R_0'$  than the previous type (compare chromium potentials  $pB$  and  $pD$  with zirconium potentials  $pB$  and  $pE$ ). Deuteron potentials  $dA$ ,  $dB$ , and  $dC$  cover a similar range of the deuteron  $VR^n$  ambiguity. Deuteron potentials  $dD$  and  $dE$  correspond to another type of deuteron potential with small  $a_d'$  and large  $W_d$  (compare with zirconium potential  $dH$ ). The results of using these various potentials in stripping calculations are shown in Figs. 12 and 13. The only large differences in the angular distributions occur when the use of deuteron potentials  $dD$  and  $dE$  is compared with the use of the other deuteron potentials. Since the experimental absolute cross section was not obtained, the angular distributions have been normalized to the  $(dB, pB)$  results shown in Fig. 11. As in the case of  $^{90}\text{Zr}(d,p)^{91}\text{Zr}$ , the effect on the  $S_l'/S_1'$  is greater with the use of various proton parameter sets (Fig. 12) than with the use of different deuteron parameter sets (Fig. 13). The spread in values of the  $S_l'/S_1'$  is seen to be a good deal less than the range of values covered by the  $S_l'$ , again indicating that the relative spectroscopic factors are somewhat more reliable than the absolute ones.

### $^{206}\text{Pb}(d,p)^{207}\text{Pb}$

Parameter sets  $dA$ ,  $dB$ ,  $pA$ , and  $pB$  yield the fits to the elastic-scattering data for 14-MeV deuterons on  $^{206}\text{Pb}$  and 17-MeV protons on Bi shown in Fig. 14. The two calculated deuteron angular distributions are quite similar, as are the two proton angular distributions.

The  $^{206}\text{Pb}(d,p)^{207}\text{Pb}$  curves 1, 2, 3, and 4 of Fig. 15 correspond to the four possible ways of combining these parameter sets in stripping calculations. The curves are seen to be quite different from one another: curves 1 and 2 are out of phase with curves 3 and 4; curve 1 differs in magnitude at large angles from curve 3, as does curve 2 from curve 4. Curves 5 and 6 correspond to the best fits obtained for these data. They in turn do not agree with curves 1, 2, 3, or 4, although the main difference between 5 and 6 and 3 and 4 is that  $R_{0d}$  and  $R_{0p}$  were increased slightly to obtain the former two. From the large range of results possible and the fact that curves 5 and 6 show a fair resemblance to the data, I concluded that if the parameter space were exhaustively searched, parameters could be found which would simultaneously fit the elastic scattering and the stripping. Some efforts were made in this direction but were abandoned short of success because (1) since the variation in results is so large, a fit to the stripping data could not be used to draw definite conclusions about the validity of the theory, and (2) as shown below, either the accuracy of the elastic-scattering data or the invariance of the average nuclear potentials to changes in mass and energy is in doubt.

The latter situation arises because two experimental determinations of  $\text{Pb}(d,d)\text{Pb}$  angular distributions for  $E_d = 15$  MeV<sup>26,27</sup> do not agree either with each other or with the present 14-MeV  $^{206}\text{Pb}(d,d)^{206}\text{Pb}$  data. Furthermore, parameters determined by calculations using 21.6-MeV  $^{206}\text{Pb}(d,d)^{206}\text{Pb}$  and 22.2-MeV  $^{208}\text{Pb}(p,p)^{208}\text{Pb}$  data (parameter sets  $dA'$  and  $pA'$  in Table II) do not

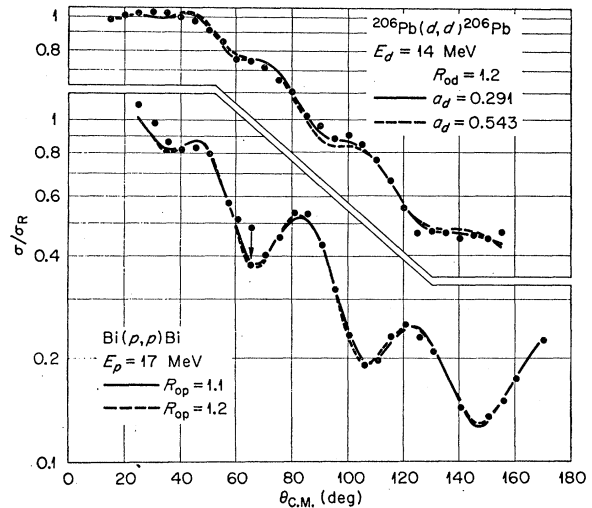


FIG. 14. Comparison between experimental and calculated angular distributions for the elastic scattering of 14-MeV deuterons on  $^{206}\text{Pb}$  and 17-MeV protons on Bi. The parameters are sets  $dA$ ,  $dB$ ,  $pA$ , and  $pB$  listed in Table II.

<sup>26</sup> N. Cindro and N. S. Wall, Phys. Rev. **119**, 1340 (1960).

<sup>27</sup> R. K. Jolly, E. K. Lin, and B. L. Cohen, Phys. Rev. **130**, 2391 (1963).

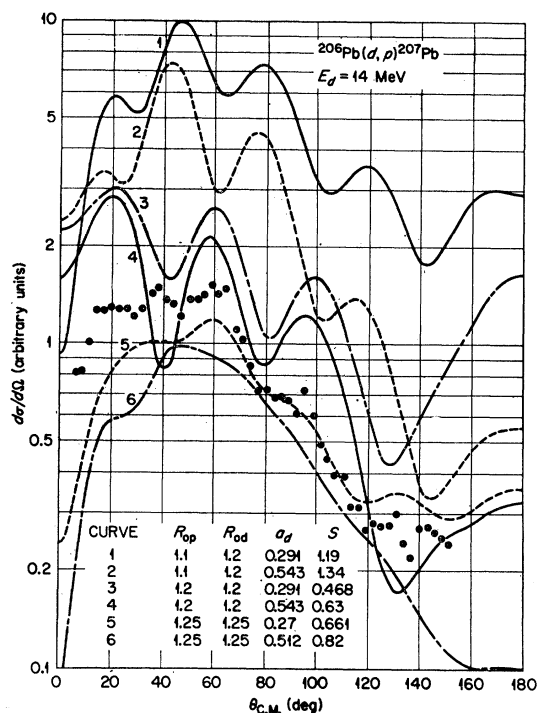


FIG. 15. Calculations for the  $E_d = 14$ -MeV,  $^{206}\text{Pb}(d, p)^{207}\text{Pb}$ ,  $l=1$  reaction leading to the ground state of  $^{207}\text{Pb}$ . The angular distributions have been arbitrarily displaced vertically relative to one another for better clarity. The parameter sets used correspond to sets  $pA$ ,  $pB$ ,  $pC$ ,  $dA$ ,  $dB$ ,  $dD$ , and  $dE$  in Table II.

agree with the parameters found from studying the 14-MeV  $^{206}\text{Pb}(d, d)^{206}\text{Pb}$  or the 17-MeV  $\text{Bi}(p, p)\text{Bi}$  data.

On the assumption that the parameter sets used in obtaining the angular distributions of Fig. 15 are the correct predictions of suitable elastic-scattering data, the results are interpreted as follows: The strong dependence on parameters indicates that much of the stripping occurs in the nuclear interior. As a test of the possibility that the absorption potentials employed are smaller than is physically correct,  $W_d$  and  $W_p$  were doubled for all the potential sets and the stripping was recalculated. The resulting curves (examples are shown in Fig. 16) varied a great deal less in shape at angles below about  $120^\circ$  than do the curves shown on Fig. 15. Also, when a radial cutoff at the radius  $R_{0p}A^{1/3}$  was used, the variation in results was again greatly reduced. Both procedures caused the stripping angular distributions to look more like the data, and especially was this true in the latter case. Curves 5 and 6 of Fig. 16 show the effects that these changes had on curves 5 and 6 of Fig. 15. These particular cases are illustrated because the cut-off results agree best with the experimental data. These studies imply the correctness of including finite-range and nonlocal potentials in the calculations, since the combined inclusion of these phenomena serves to reduce the interior contributions to the stripping integrals by about 50%, an effect which can be simu-

lated by using radial cutoffs. Making the imaginary potentials larger also reduces the interior contributions, but unlike using a cutoff or finite-range and nonlocal potentials, this procedure also affects the nuclear wave functions, and hence the radial integrals, in the exterior region.

### Zn( $d, p$ )

The deuteron elastic-scattering studies of Halbert<sup>8</sup> and the proton and deuteron studies of Perey<sup>7</sup> usually exhibit several sets of parameters which explain a given set of data. Since they investigated both 11.8-MeV deuteron data and 17-MeV proton data, using zinc as the target, I decided to make calculations of a hypothetical isotope having the mass and charge of natural zinc and having  $l=1, 2$ , and 4 ( $d, p$ ) transitions such that 11.8-MeV incident deuterons yield 17-MeV protons. The results are shown in Fig. 17, where the  $S_i'$  are extracted on the assumption that the stripping results ( $pA, dC$ ) are the data. As in the  $^{90}\text{Zr}(d, p)^{91}\text{Zr}$  and  $^{52}\text{Cr}(d, p)^{53}\text{Cr}$  investigations, the results indicate that the angular distributions are not particularly sensitive to the choice of parameters, that different proton radii create sizable differences in the resulting spectroscopic factors and that the  $S_i'$  decrease with increasing  $R_{0p}$ , and that the relative spectroscopic factors show less variations than the absolute ones.

Curve ( $pB, dB$ ) corresponds to the use of a deuteron potential very similar to  $dA$  except for the value of  $V_d$ . The resulting oscillations in the  $l=1$  angular distribution<sup>20</sup> are out of phase with the preceding results, although the average slope is the same. The ( $pB, dA$ ) curve fits reasonably well some experimental 11.9-MeV,  $l=1$ ,  $^{68}\text{Zn}(d, p)^{69}\text{Zn}$  data.<sup>28</sup> Similar presumably  $l=2$  and 4 data are not fitted by any of the calculations, a result also found in a previous investigation.<sup>4</sup>

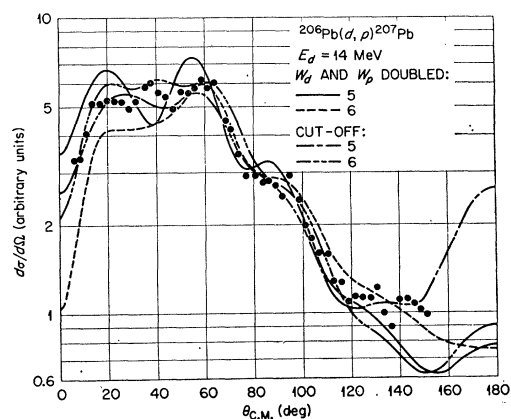


FIG. 16. Recalculations of curves 5 and 6 of Fig. 15 in which in one case both the deuteron and proton imaginary potential depths have been doubled and in the other case the radial integration has  $R_{0p}A^{1/3}$  as its lower bound.

<sup>28</sup> F. S. Eby, Phys. Rev. **96**, 1355 (1954).

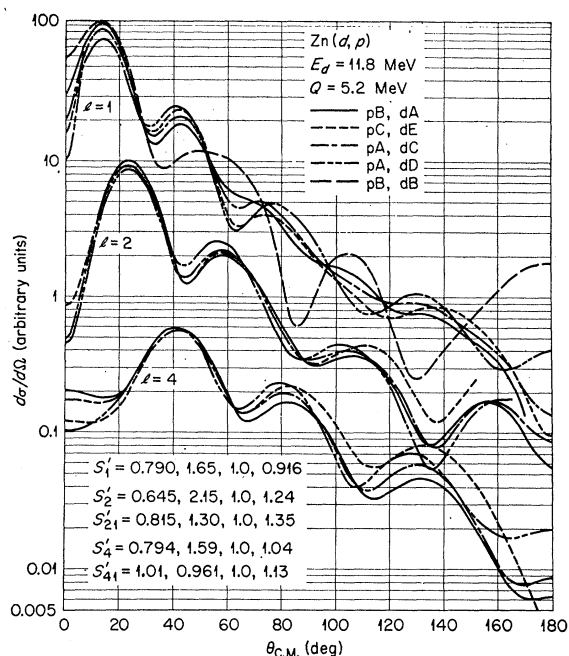


FIG. 17.  $(d, p)$  calculations for a target assumed to have the mass and charge of natural zinc.

### SUMMARY

Three major conclusions deserve mention, and are discussed below: (1) The spectroscopic factors are not reliably determined by DWBA calculations; (2) the present theory appears to explain rather well the  $(d, p)$  relative angular distributions for medium weight targets; and (3) more accurate and more complete data for DWBA stripping studies should be made.

(1) The absolute spectroscopic factors determined here vary by more than a factor of 2 when the range of acceptable elastic-scattering parameter sets is traversed. The relative spectroscopic factors for different  $l$ -value transitions are about twice as dependable as the absolute ones.

(2) The fact that the stripping theory appears valid for medium-weight nuclei is indicated by the quality of fits obtained here and by the lack of appreciable dependence of the angular distributions on parameters in the cases of the  $^{90}\text{Zr}(d, p)^{91}\text{Zr}$  and  $^{52}\text{Cr}(d, p)^{53}\text{Cr}$  reactions. For the latter reaction this agreement is seen to persist over a range of energies, and in particular it indicates that the DWBA theory is valid for bombarding energies well below the Coulomb barrier energy. The  $^{206}\text{Pb}(d, p)^{207}\text{Pb}$  investigation yielded inconclusive results as to the applicability of the theory to heavy nuclei. Studies of light-nuclei stripping are still in progress but have not yet indicated that the present  $(d, p)$  calculations are suitable for light targets. Even the favorable  $^{90}\text{Zr}(d, p)^{91}\text{Zr}$  results, and especially the  $^{52}\text{Cr}(d, p)^{53}\text{Cr}$  results, must be viewed with caution because of the uncertainty in the normalization chosen

for the elastic-scattering data. This points up the need for having complete sets of data when making DWBA calculations.

(3) Several additional stripping reactions could have been studied here had the prerequisite deuteron and/or proton elastic-scattering data been available. In other cases the elastic-scattering data were available, but the stripping data extended over too small a range of angles to be very useful. Even the  $^{90}\text{Zr}(d, p)^{91}\text{Zr}$  data treated here were of limited usefulness since large errors were present in the relative angular distributions and only stripping distributions leading to two final states were definitely resolved. With complete and accurate data, discrepancies between an experiment and any theory used to explain it will show up more clearly, and progress in improving the theory will be correspondingly enhanced.

Other results of somewhat lesser importance than the preceding are that ambiguities in the real potential radii affect the stripping more seriously than other potential ambiguities, that if the imaginary potentials are sufficiently large then the stripping results show a qualitative similarity to one another, and that there is often a considerable correlation between the imaginary parameters  $R_0'$  or  $a'$  and  $W$  such that if one of them is changed appreciably then the other can be changed in compensatory fashion so as to maintain the agreement with the elastic-scattering data. It has been shown that among the parameters the choice of radii is the most critical in determining angular distributions and that the choice of proton (or neutron) radius is in particular of greatest importance for the extraction of spectroscopic factors—especially if the neutron form factor is constrained to be identical to the proton form factor. Hence in any realistic comparison with experiment, stripping calculations should be made which extend throughout the range of possibly acceptable radii in order to estimate the size of the error caused by the uncertainty in radius.

Turning now to variations in the results, the  $^{90}\text{Zr}$ ,  $^{52}\text{Cr}$ , and Zn stripping calculations indicate that, if the imaginary potentials are reasonably large, then over considerable variations within the acceptable parameter space the stripping angular distributions are mutually similar in gross features. Hence if detailed fits to the data are not demanded, the use of any reasonable set of acceptable parameters (provided the correct potential depth is employed) will indicate whether or not the theory is capable of yielding agreement with experimental stripping angular distributions. This is not true regarding the spectroscopic factors, nor is it valid when the imaginary potential strengths are anomalously small.

Finally, in addition to the well-known  $VR^n = \text{constant}$  ambiguity for the real potential and also to the ambiguity characterized by letting the "constant" in this equation take different discrete values, there exists an

ambiguity in the imaginary potential parameters. If the imaginary potential parameters are allowed to be correlated not only among themselves but also with the real radius  $R_0$ , two different absolute minima of the best-fit criteria  $X$  in the parameter space can be found for the cases  $Zr(d,d)Zr$ ,  $^{52}Cr(d,d)^{52}Cr$ , and  $^{206}Pb(d,d)^{206}Pb$ . The differences in the stripping results for the chromium reaction were sufficiently large that the deuteron potential with the smaller real radius could be chosen as the one more likely to be correct.

Additional means for improving calculations become apparent from this work:

(1) The  $^{90}Zr(d,p)^{91}Zr$  results indicated that only one type of imaginary potential form factor (e.g., either Woods-Saxon, derivative, or Gaussian) need be tried in stripping calculations.

(2) The  $^{206}Pb(d,p)^{207}Pb$  results showed that in taking data for distorted wave analysis the bombarding energy should be high enough for the angular structure of the elastic scattering to be well defined. The strong dependence of the lead results on the choice of parameters may have been due in part to the fact that the relatively greater volume-to-surface ratio of heavy targets might have caused  $(d,p)$  calculations for them to be more dependent on the nuclear interior. Furthermore,  $^{206}Pb$ , being near a doubly magic nucleus, may have a lower density of compound levels and hence a smaller rate of incident particle absorption, with the consequence that the relative importance of stripping from the interior is increased.

(3) The  $^{52}Cr(d,p)^{53}Cr$  results suggested that some form of spin-orbit or tensor interaction should be included in the calculations.

(4) Comparison of the  $^{206}Pb(d,d)^{206}Pb$  results at 14

and at 21.6 MeV and comparison of the  $Bi(p,p)Bi$  results at 17 MeV with the  $^{208}Pb(p,p)^{208}Pb$  results at 22.2 MeV indicated that the optical model may not always give consistent parameters when different energy data are used. Hence in evaluating stripping results elastic parameters obtained at several different energies should be considered if possible.

(5) Errors in the elastic proton normalization appear to generate errors of like size in the resulting spectroscopic factors. Moderate errors in the normalization, especially the normalization of the proton scattering, do not appear to affect seriously the relative stripping angular distributions.

Since  $(d,p)$  reactions are probably the simplest type of rearrangement collision to handle theoretically, an understanding of their mode of operation should be a prerequisite for understanding more complicated reactions. However, before significant improvements in the theory can be expected, better and more complete sets of data for use in checking the theory will have to become available. A final solution to the problem of obtaining reliable spectroscopic factors will probably be difficult to obtain, if for no other reason than that the spectroscopic factors are strongly dependent on the normalization of the neutron radial wave function and that this normalization is in turn critically influenced by the imprecisely known form of the neutron-target interaction.

#### ACKNOWLEDGMENTS

The author is grateful to F. G. Perey and G. R. Satchler for sharing their knowledge of nuclear processes, and to the latter for a critical reading of the manuscript.